ELSEVIER

NeuroToxicology 25 (2004) 555–572

NeuroToxicology

Selective Changes in Gene Expression in Cortical Regions Sensitive to Amphetamine During the Neurodegenerative Process

John F. Bowyer[1,*], Angela J. Harris[1], Robert R. Delongchamp[1], Robert L. Jakab[1], Diane B. Miller[2], A. Roger Little[2], James P. O'Callaghan[2]

[1]*Divisions of Neurotoxicology, Biometry and Risk Assessment and Genetic Toxicology, National Center for Toxicological Research, Jefferson, AR 72079, USA*

[2]*Centers for Disease Control and Prevention-NIOSH, 1095 Willowdale Road, Morgantown, WV 26505, USA*

Received 1 May 2003; accepted 7 August 2003

Available online 9 October 2003

Abstract

Gene expression profiles in several brain regions of adult male rats were evaluated following a D-amphetamine (AMPH) exposure paradigm previously established to produce AMPH neurotoxicity. Escalating doses of AMPH (5–30 mg/kg) were given over the course of 16 h per day in an 18 °C environment for 2 days. This paradigm produces neurotoxicity but eliminates or minimizes the hyperthermia and seizure activity that might influence gene expression in a manner unrelated to the neurotoxic effects of AMPH. The expression of 1185 genes was monitored in the striatum, parietal cortex, piriform cortex and posteriolateral cortical amygdaloid nucleus (PLCo) using cDNA array technology, and potentially significant changes were verified by RT–PCR. Gene expression was determined at time points after AMPH when neurodegeneration was beginning to appear (16 h) or maximal (64 h). Expression was also determined 14 days after AMPH to find long-term changes in gene expression that might be biomarkers of a neurotoxic event. In the parietal cortex there was a two-fold increase in neuropeptide Y precursor protein mRNA whereas nerve growth factor-induced receptor protein I-A and I-B mRNA decreased 50% at 16 h after the end of AMPH exposure. Although these changes in expression were not observed in the PLCo, insulin-like growth factor binding protein 1 mRNA was increased two-fold in the PLCo at 16 and 64 h after AMPH. Changes in gene expression in the cortical regions were all between 1.2- and 1.5-fold 14 days after AMPH but some of these changes, such as annexin V increases, may be relevant to neurotoxicity. Gene expression was not affected by more than 1.5-fold at the time points in the striatum, although 65% dopamine depletions occurred, but the plasma membrane-associated dopamine transporter and dopamine D2 receptor were decreased about 40% in the substantia nigra at 64 h and 14 days post-AMPH. Thus, the 2-day AMPH treatment produced a few changes in gene expression in the two-fold range at time points 16 h or more after exposure but the majority of expression changes were less than 1.5-fold of control. Nonetheless, some of these lesser fold-changes appeared to be relevant to the neurotoxic process.

Keywords: Amphetamine; Gene expression; Neurodegeneration

INTRODUCTION

The current studies employed a rat model of AMPH neurotoxicity that produce neurodegeneration independent of hyperthermia, seizures, or stroke to look for short- and long-term changes in gene expression that may occur within the damaged brain regions. It is important to characterize such a paradigm because it may more closely model the neurotoxicities produced in the human population exposed to high doses of AMPH, when severe hyperthermia, seizures or stroke are not a factor. Determining the changes in

* Corresponding author. Tel.: +1-870-543-7194; fax: +1-870-543-7745.
E-mail address: jbowyer@nctr.fda.gov (J.F. Bowyer).

0161-813X/$ – see front matter © 2003 Elsevier Inc. All rights reserved.
doi:10.1016/j.neuro.2003.08.005

gene expression specifically due to AMPH is confounded if significant hyperthermia, seizures or stroke are concomitant with AMPH exposure since all of these physiological factors can alter gene expression effects in the absence of AMPH (Westman and Sharma, 1998; Tang et al., 2001; Bates et al., 2001; Kiessling and Gass, 1993; Gall, 1993; Chen et al., 2001). The elimination of these factors in the present study helps to ascertain more precisely what might be truly AMPH-induced changes in gene expression within brain regions where moderate neurotoxicity results from AMPH exposure.

AMPH and METH exposure can clearly produce signs of neurotoxicity in laboratory animals including extensive dopamine depletions in the caudate/putamen, neurodegeneration in several sensory and limbic-related cortical regions, thalamic neurodegeneration and short-term motor-activity deficits (Bowyer and Holson, 1995; Bowyer et al., 1998; Davidson et al., 2001; O'Callaghan and Miller, 2001; Seiden and Sabol, 1995). The types of neurotoxicity produced by these compounds in humans and the degree to which they produce a similar neurotoxicity in humans compared to laboratory animals are still being evaluated (Ernst et al., 2000; McCann et al., 1998; Wilson et al., 1996; Volkow et al., 2001a,b). However, it does appear that some loss of striatal dopaminergic and cortical function and impairment of some types of cognitive function occur after chronic METH abuse (McCann et al., 1998; Volkow et al., 2001a,b).

In the acute paradigms, either four doses of AMPH or METH (ranging from 5 to 15 mg/kg) are administered with a 2 h interval between each dose (Sonsalla et al., 1989) or a single high dose of 40 mg/kg or greater is given (Cadet et al., 2001; Xie et al., 2002). Although these exposure paradigms have some advantages over the chronic dosing paradigms, they all produce significant hyperthermia that greatly influences AMPH and METH neurotoxicity (Bowyer et al., 1992, 1994; O'Callaghan and Miller, 1994). In addition, at initial doses of 15 mg/kg or greater, both AMPH and METH often induce seizure activity that results in behavioral symptoms of status epilepticus lasting for more than an hour (Bowyer et al., 1998; Bowyer, 2000, unpublished data).

Previous studies looking at the changes in gene expression after exposure to neurotoxic doses of amphetamine-related compounds have focused on METH-induced changes produced in experimental paradigms that employ single injections or acute neurotoxic dosing in mice (Cadet et al., 2001; Xie et al., 2002). These dosing paradigms are known to produce pronounced hyperthermia and seizures in mice, and as previously cited their occurrence can confound the interpretation of the role of METH (or AMPH) in the changes in gene expression. Also, only relatively short time periods of several hours to 24 h after METH exposure were primarily monitored to determine changes in gene expression in previous studies.

We have been actively evaluating alternative AMPH and METH dosing paradigms in the mouse and rat that have the potential to produce neurotoxicity in the absence of hyperthermia, seizures as well as stroke (Bowyer et al., 2001; Jakab and Bowyer, 2002). Our present studies used a 2-day AMPH exposure paradigm, conducted at a lowered environmental temperature (17–18 °C) that can produce neurotoxicities in the cortex and striatum without inducing hyperthermia or seizures (Jakab and Bowyer, 2002). Thus, this model provides an opportunity to evaluate changes in gene expression after AMPH exposure without the confounding influence of hyperthermia, seizures or stroke.

Both the short-term (16 and 64 h) and long-term (14 days) changes in the gene expression within brain regions damaged by the 2-day AMPH exposure were evaluated. The Clontech Atlas 1.2 K array was chosen for this study because it uses gene specific primers in the reverse transcription (RT) step. To further characterize the neurotoxicity that may occur in the striatum from 2-day AMPH, we have evaluated dopamine, tyrosine hydroxylase (TH) and GFAP levels at the three time points after AMPH exposure.

MATERIALS AND METHODS

Animal Housing Conditions and Dosing

All the procedures involving animals were approved by the Institutional Animal Care and Use Committee of the NCTR, and the studies were carried out in accordance with the declaration of Helsinki and the Guide for the Care and Use of Laboratory Animals as adopted and promulgated by the National Institutes of Health. Prior to dosing, the 4- to 6-month-old male Sprague–Dawley rats used in the experiments were housed in a vivarium on a 12 h daily light cycle with lights on 6.00 a.m. The temperature (22–23 °C) and humidity (53 ± 15%) were controlled with food and water available ad libitum. One day prior to testing the

rats were placed 1 per cage in a 17–18 °C environment.

The rats were administered gradually increasing doses of either AMPH subcutaneous (s.c.) or 1 ml/kg s.c. normal saline for 16 h per day for 2 days using the dosing schedule shown as follows:

	1st dose (8.00 a.m.)	2nd dose (10.00 a.m.)	3rd dose (12.00 p.m.)	4th dose (4.00 p.m.)	5th dose (8.00 p.m.)	6th dose (12.00 a.m.)
1st day (mg/kg)	5	5	5	15	15	30
2nd day (mg/kg)	5	7.5	10	15	15	30

The body temperatures were monitored at 1 h after the 1st, 2nd and 3rd dose and 1 and 2 h after each of the last three doses. The core body temperatures were determined using a rectal thermistor as described by Bowyer et al. (1994). When an animal's body temperature exceeded 38.7 °C, it was placed in a clean and dry cage resting on crushed ice for 30 min to prevent its temperature from rising above 39.0 °C. If the body temperature exceeded 39.5 °C, the rat was placed directly on crushed ice for 15–25 min until the body temperature fell below 38.0 °C to prevent its temperature from rising above 39.9 °C. Behaviors were monitored and recorded during dosing at 30 min intervals. Since animals administered AMPH did not eat or drink water from 8.00 a.m. to 1.00 a.m., access to food and water was denied the saline controls during this interval. Also, the food consumption of the AMPH-treated rats was decreased to about of 10 g per day during AMPH exposure. Therefore, the controls' daily food intake was limited to this level until 2 days post-dosing, when food consumption returned to near normal in AMPH-treated rats.

In the studies presented herein, 42 rats were used for cDNA array analysis as well as striatal dopamine, TH and GFAP levels after the 2-day AMPH exposure. The animals used to determine the changes in gene expression in the present study were administered AMPH and sacrificed concurrently with the animals used for histological evaluation of neurotoxicity (previously reported by Jakab and Bowyer, 2002) in which prominent neurodegeneration was detected in the parietal cortex and posteriolateral cortical amygdaloid nucleus (PLCo). Thus, neurotoxicity should have been produced by AMPH in the parietal cortex and PLCo tissues used to generate total RNA for the gene expression studies. In addition, 20 rats were exposed to the 2-day dosing paradigm, as a follow up study to histologically verify overt changes in the distribution and density of protein products of several genes whose expression was affected by (data in Figs. 3 and 4).

Sacrifice and Tissue Harvest for cDNA Array Data Collection

Six saline-treated and six AMPH-treated animals were sacrificed for the 16 and 64 h post-dose time point for each time point while 12 saline-treated and 12 AMPH-treated animals were sacrificed for the 14-day post-dosing time point. Animals were sacrificed by decapitation, and their brains were rapidly removed and chilled in 4 °C normal saline. The striatum, parietal cortex, PLCo and substantia nigra tissues were dissected bilaterally on ice, immediately frozen on dry ice, and remained there for less than 2 h before being transferred to −70 °C storage. Parietal cortex was harvested, 40–50 mg per hemisphere, between −0.0 and −2.5 anterior–posterior coordinates according to Paxinos and Watson (1995) while PLCo and adjacent ventral piriform cortex, 9–15 mg per hemisphere, was dissected between −2.3 and −3.6 anterior–posterior. For each animal one striatum, 45–55 mg, tissue from one hemisphere was used for determining the levels of dopamine, serotonin (5-HT) and their metabolites as well as TH levels and glial fibrillary acidic protein. The contralateral striatum was used for isolating total RNA. Approximately 35–45 mg of substantia nigra and surrounding tissue, primarily pyramidal tracts with minimal ventral tegmentum, was isolated per animal. Tissue from the parietal cortex and the substantia nigra from both hemispheres were used to isolate total RNA.

RNA Isolation and cDNA Array Analysis

Methods similar to those described by Freeman et al. (2000; 2001a,b) were used to isolate total RNA from brain tissue and hybridize the ^{32}P-cDNA generated from this total RNA with cDNA macro array screens.

Total cellular RNA was first isolated using Tri Reagent™ (Molecular Research Center Inc., Cincinnati, OH) by the procedure of Chomczynski (1993, 1995) which minimizes the genomic DNA contamination in the isolated total RNA. The total RNA was further purified by re-suspension in 200 μl diethyl pyrocarbonate (DEPC)-treated H_2O and re-precipitated with 20 μl 3 M NaOAc and 75% ethanol. The RNA pellet was washed once with 70% ethanol and once with 100% ethanol, and the final RNA pellet was re-suspended in 20–35 μl of DEPC-treated water. RNA levels in the aliquots were quantified using the Agilent 2100 Bioanalyzer using the RNA 6000 Nano Assay (Agilent Tech., Palo Alto, CA). The final total RNA levels ranged from 2.5 to 3.5 μg/μl, and were stored at −70 °C.

The procedures used to evaluate gene expression using the Clontech Atlas 1.2 K rat array (Cat. # 7854) were those suggested by Clontech (Clontech; Palo Alto, CA). Two significant alterations in the procedures were PowerScript™ (Clontech) was used as the reverse transcriptase polymerase and the denatured sheared salmon testes DNA and sheared mouse DNA enriched for repetitive sequences (Cot-1 DNA; Invitrogen Corp., Carlsbad, CA) were added to the hybridization buffer before pre-hybridization of the array membranes with the buffer. A 20 μl volume reaction was used for the RT step producing the cDNA target necessary for hybridization with the array membrane ''probes'', which included 6 μl of (α-^{32}P)-dATP with a specific activity of 10 μCi/μl (370 MBq/ml); 3000 Ci/mmol; New England Nuclear, Boston, MA. Seven micrograms of total RNA (a volume of between 2 and 3 μl of total RNA aliquot was added to the reaction depending on the aliquot concentration) was hybridized with 2 μl of target specific mRNA primers (10 μM) and the volume was adjusted to 5 μl with RNase free water if necessary. After incubation at 70 °C for 2 min, the primed total RNA was added to 15 μl of RT mix. The 20 μl RT mix contained (final concentration) 500 μM dCTP, 500 μM dGTP, 500 μM dTTP, 50 mM Tris–HCl (pH 8.3), 75 mM KCl, 3 mM $MgCl_2$, 5 mM DTT and 6 μl ^{32}P-dATP and 1.5 μl (150 units) PowerScript™. The RT reaction was carried out at 49 °C for 30 min, and was terminated using 10 mM EDTA (final concentration). Preparation and hybridization of the ^{32}P-labeled targets for control and AMPH aliquots for the same bran brain region and time point were always processed in simultaneously (same day, same reactants except for total RNA) in pairs to minimize the variability ^{32}P incorporation into the target.

The unincorporated ^{32}P was removed from the cDNA targets using NucleoSpin™ extraction columns and procedures provided by Clontech. The purified cDNA targets were eluted from the spin columns in 100 μl aliquots and denatured by the addition of 11 μl of a 1 M NaOH and 10 mM EDTA solution and incubation at 68 °C for 20 min. This reaction was then neutralized by the addition of 115 μl of 1 M NaH_2PO_4, pH 7.0 and 10 min incubation at 68 °C. The nylon array membranes were wetted with deionized water for 5 min, and then placed in glass cylindrical containers (4 cm diameter and 15 cm in length with screw caps). They were placed in a Hybaid (Franklin, MA) rotary incubator and pre-hybridized at 68 °C for 1–2 h in a solution containing solution containing 5 ml of ExpressHyb, 50 μl sheared salmon testes DNA (denatured just prior to addition) and 5 μl Cot-1 rat DNA. The ^{32}P-dATP-labeled targets were then added to the array membrane and pre-hybridization solution and rotary hybridization at 68 °C continued for 8–10 h (overnight).

The hybridized arrays were then rotary-washed at 68 °C. First 3× (for at least 30 min each) with 100 ml of 2× SSC and 1% SDS, and then washed 1× for 45 min with 0.1× SSC and 0.5% SDS. They were then washed for 5 min in 2× SSC, and then immediately wrapped in plastic and exposed on phosphor image screens for 1–3 days and then the screen radioactive profile determined using the PhosphorImager system from Molecular Dynamics (Sunnyvale, CA). The membranes were processed for reuse in hybridization assays as described by Clontech except that membrane stripping was accomplished by placing the membranes in 95 °C (not 100 °C) sterile water containing 0.5% sodium dodecyl sulfate for 5 min with gentle agitation.

Analysis of cDNA Arrays for Gene Expression

The binding of the radiolabeled targets to the array probes was visualized/detected by exposing the arrays on PhosphorImager plates (Molecular Dynamics) for 1–3 days. The phosphorescent images were then read using a Storm 860 PhosphorImager (Molecular Dynamics), and the targets hybridization to various membrane probes was quantified using the AtlasImage 2.0 software provide by Clontech. The arrays from AMPH-treated animals were not used for data collection if they had an incorporated radioactivity level more than two-fold different than from the control arrays that they were processed in parallel with.

Statistical Analysis of cDNA Arrays

All statistical analyses were conducted on the logarithm (base 2) of normalized intensities. The procedure is similar to a median global normalization except it is based upon two quantiles, the 10th and 75th. The observed intensities were normalized by a multiplicative alignment of the 0.75 quantile and an additive alignment of the 0.10 quantile. Ostensibly, the multiplicative alignment copes with differentials in scale factors among arrays and the additive alignment copes with differentials in the background. The details are given elsewhere (Delongchamp et al., 2003).

Effects attributable to amphetamine treatment were assessed within the samples from the PLCo and the parietal cortex. An analysis of variance on the normalized data estimated the effect of treatment within blocks that consisted of an amphetamine sample and a saline sample processed concurrently. Some rats were assayed on more than one array, but because of block effects it is not valid to average across arrays. The variation attributed to rats was small relative to the variation attributed to arrays. So the analyses treated arrays as if they were the experimental units instead of the rats; therefore, all of the data were usable. Conceptually, this 'approximation' will underestimate the variance of treatment differences and overestimate their significance although we believe this bias is negligible. Blocks were nested within sacrifice times and treatment differences were estimated for each sacrifice time. This analysis was implemented using SAS (SAS Institute Inc., Cary, NC, 1999).

The estimate of the treatment effect within each sacrifice time is an estimate of the logarithm (base 2) of the fold change: amphetamine/saline. Estimates were computed for each gene, sacrifice time and brain region. To manage the large number of comparisons, the 1185 interrogated genes were partitioned into two groups for each brain region: expressed genes and low/unexpressed genes. Conceptually, treatment differences in expression cannot occur if the gene is not expressed. This partitioning was based upon the distribution of the average over arrays of log-intensities for each spot within a brain region (Delongchamp et al., 2003; Lee et al., 2000). The P-values (actually $1 - p$) were plotted against their expectation assuming a uniform distribution (Schweder and Spjotvoll, 1982). From this plot, the number of true null hypotheses was assessed, and the false discovery rate was estimated (Benjamini and Hochberg, 2000; Delongchamp et al., 2003; Storey, 2002).

RT–PCR Verification of Fold-Changes

The same aliquots of total RNA, from the various brain regions, used to generate the cDNA array targets were diluted to 0.4 μg total RNA/μl DEPC-treated water for use in the reverse transcription (RT) phase of the RT–PCR. The RT reaction was run using the standard techniques optimized for use with Superscript™ II reverse transcriptase (Invitrogen Corp.). Random hexamers (0.2 μg) were used for priming 0.8 μg of total RNA in a 20 μl reaction mixture that also contained 400 μM dNTPs. This mixture was incubated at 65 °C for 5 min, and then the samples were placed on ice for more than 5 min. The RT reaction was then initiated by adding 20 μl of the reaction mixture to the original 20 μl priming mixture. The final concentrations of reactant constituents were 20 mM Tris–HCl (pH 8.4), 50 mM KCl, 5 mM $MgCl_2$, 10 mM dithiothreitol, 200 μM dNTP, 0.5 units/ul RNase inhibitor and 2.5 units Superscript™ II RNase H^- (Invitrogen Corp.) reverse transcriptase polymerase. The reactants were first incubated for 10 min at 25 °C then 40 °C for 50 min, followed by 70 °C for 15 min.

The real-time polymerase chain reaction (PCR) methods used were those for the iQ™ SYBR® Green Super mix (Bio-Rad Labatories, Hercules, CA) for generating a FAM 490 fluorescent product. The final concentrations of the various reactants in the 50 μl PCR reaction mixture were; 50 mM KCl, 3 mM $MgCl_2$, 20 mM Tris–HCl (pH 8.4), 200 μM dNTP, 2.5 units/50 μl of iTaq DNA polymerase, SYBR Green I, 100 nM fluorescein and 2 μl of RT product. The primers were used at 200 nM concentrations, and the primer sequences for the particular mRNA species evaluated are shown below. All primers had annealing temperatures between 55 and 60 °C, and only the DAT and 28S primers did not span introns.

mRNA species	Position of primers	Sequence of 5′ and 3′ primers
28S	5′ at 6490	5′-TATCCGCAGCAGGTCTCCAAG-3′
	3′ at 6589	5′-GACCGACCCAGCCCTTAGAGC-3′
GAPDH	5′ at 517	5′-CATGACAACTTTGGCATCGTG-3′
	3′ at 595	5′-GCCACAGCTTTCCAGAGGG-3′

mRNA species	Position of primers	Sequence of 5′ and 3′ primers
NPY-P	5′ at 45	5′-CGCCATGATGCTAGGTAACA-3′
	3′ at 173	5′-ATCTGGCCATGTCCTCTGCTG-3′
(EGR-1) NGFI-A	5′ at 512	5′-GGCAGCAGCGCTTTCAATCCT-3′
	3′ at 598	5′-CCAGCGCCTTCTCGTTATTC-3′
IGFBP-1	5′ at 1310	5′-GGGGAGACTTCCTCATCGAAT-3′
	3′ at 1411	5′-GTTTAACAGTGCATGGGACGC-3′
DAT	5′ at 279	5′-GTCATCGGCTTTGCTGTGGAC-3′
	3′ at 349	5′-GTAGGGCACCAGGAAGGCAC-3′
TH	5′ at 475	5′-ACGTGCGCAGTGCCAGAGAGG-3′
	3′ at 579	5′-AAGCCCGGGTGGTCCAG-3′
GFAP	5′ at 464	5′-GGCACCCTGAGGCAGAAG-3′
	3′ at 590	5′-GATCTCCTCCTCCAGCGACTCT-3′

Product was generated in 96-well plates, containing 50 μl of the PCR reaction mixture per well using a program consisting of 4 min at 95 °C to activate iTaq polymerase followed by 40 cycles of amplification consisting of 20 s at 95 °C coupled to 30 s at 55 °C. Upon completion of the PCR amplification cycles one cycle of 1 min at 95 °C followed by 1 min at 55 °C the temperature was increased at 0.5 °C every 10 s to generate a melting curve for the PCR products. Excitation was elicited with a 490 ± 10 nm wave-length, and the emission detected at 530 ± 10 nm wave-length was used to monitor the formation of fluorescent PCR products. The relative levels of various species of mRNA in the aliquots were determined by the number of cycles to reach threshold of detection as described for the ABI Prism 7700 Sequence Detection System in User Bulletin #2 (ABI; Foster City, CA). Specificity of PCR product for the various primers was verified using the melt curves of the PCR products.

Data from the RT–PCR experiments are summarized in Table 2 by showing the cycles to optical threshold (2nd column) for each gene in RNA obtained from either control or AMPH-treated animals. C_t values for the various genes were adjusted/normalized (shown in 3rd column) by subtracting from them the respective C_t values of GAPDH (''house keeping'' gene) derived from the same aliquot (same time point and brain region) from them. The ''normalized'' difference between the control and AMPH-treated are then generated by subtraction (4th column). A value of 1.0 would mean that it took one more cycle for the AMPH group to reach the C_t compared to the control meaning that the particular mRNA species in the AMPH group was only 50% of control. A value of 1.0 would mean that the mRNA levels in the AMPH group were 200% of control (User Bulletin #2 for the ABI Prism 7700 Sequence Detection System; ABI).

Analysis of GFAP, TH and Aromatic Monoamine Levels in Striatum

To determine dopamine, 5-HT, TH, and GFAP levels, one striatum from each animal was placed in ice-cold 0.05 M sodium phosphate buffer at pH 3.0 (10× buffer volume to tissue wt.), and homogenized by ultrasonication for 30 s. For the 64 h and 14 days analysis of the dopamine, TH and GFAP levels all six control and AMPH-treated animals for both time points were determined. Samples were immediately placed on ice and split into aliquots. One aliquot, which was used for determining TH and GFAP levels, was immediately frozen on dry ice and maintained at −70 °C until analysis. The other aliquot was further acidified with a measured volume (20%, w/v) of 0.2 M perchloric acid, frozen on dry ice, and stored at −70 °C until analysis with high-pressure liquid chromatography (HPLC). The HPLC and electrochemical detection method used for quantifying dopamine, 5-HT and metabolite levels were similar to that described by Stephans and Yamamoto (1994). The HPLC retention times were 3.25 min (DOPAC), 4.7 min (dopamine), 5.95 min (5-HIAA), 10.4 min (HVA), 13.1 min (5-HT) and 15.4 min (3-methoxytyramine).

To determine TH and GFAP levels, the remaining non-HPLC aliquot was split. TH (holoenzyme protein) was assayed according to a modification of the detergent-based sandwich ELISA of O'Callaghan (1991) and Reinhard and O'Callaghan (1991). Briefly,

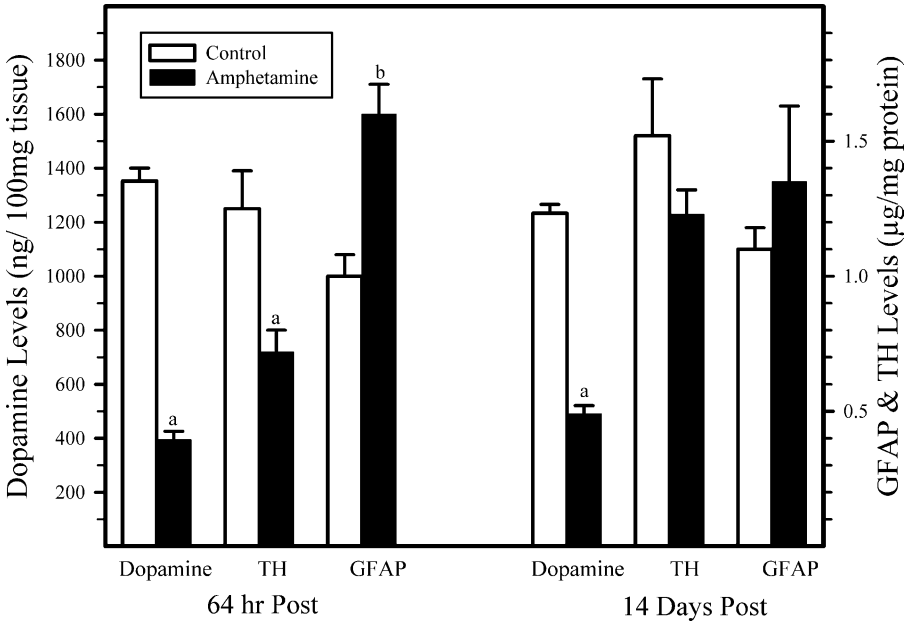

Fig. 1. Striatal dopamine, TH and GFAP depletions at 64 h and 14 days post-AMPH. The dopamine, TH and GFAP levels are shown for the striatum at 64 h and 14 days after either saline (empty bars) or AMPH (filled bars) administration. There were 10 control and 19 AMPH animals in the groups at the 64 h time point and 11 control and 17 AMPH animals in the groups at the 14-day time point. See RESULTS section for more details on the ANOVA analysis. The letter 'a' indicates levels were significantly less than control ($P < 0.05$) and 'b' indicates levels were significantly greater than control ($P < 0.05$).

a mouse monoclonal antibody to TH (Calbiochem–Novabiochem Corp., San Diego, CA) and a rabbit polyclonal antibody to TH (Calbiochem-Novabiochem Corp.) were used to ''sandwich'' TH present in detergent homogenates of brain regions. Quantification was achieved with a fluorescent substrate, Quantablu Substrate (Pierce, Rockford, IL) generated by an HRP-conjugated secondary antibody using a Fmax plate reader (Molecular Devices Corp., Sunnyvale, CA) set at 320/405 nm. TH levels were expressed as µg/mg of protein in Fig. 2. Protein levels were determined by the methods of Smith et al. (1985). Aliquots of the SDS-homogenates were assayed for GFAP using the sandwich ELISA developed in this laboratory (O'Callaghan, 1991, 2002). IgG was assayed from the same SDS-homogenates using a highly sensitive fluorescence-based ELISA adapted from the GFAP assay (O'Callaghan, 1991, 2002). Briefly, a rabbit anti-mouse IgG (Sigma Chemical Co., St. Louis, MO, Cat. # M9637) was used to capture IgG from dilutions of the SDS-homogenates followed by incubation with a goat anti-mouse IgG detection antibody (Boehringer Mannheim, Cat. # 605208). Quantification was achieved using anti-goat antibody conjugated with horseradish peroxidase with Quantablu Substrate (Cat. # 31402) as the substrate. The IgG standard was obtained from Roche (Cat. # 605208, Indianapolis, IN). Values were generated with an Fmax Plate Reader (Molecular Devices Corp.) set at 405 nm. Total protein content of the homogenates was assayed by the method of Smith et al. (1985).

Data for body temperature, dopamine, TH and GFAP levels are presented as arithmetic mean ± S.E.M. unless otherwise indicated. Multiple groups were analyzed by a two-way analysis of variance (ANOVA) (Fig. 1) using a post-hoc Tukey's least significant difference test if significant main effects were observed. To determine whether dopamine, TH or GFAP levels correlated with body temperature during AMPH dosing a Pearson product moment correlation coefficient was determined.

Histological Analysis of Cortical Regions

For immunohistological analysis of changes in the expression or distribution of NPY and IGFBP-1 immunoreactivity, animals were sacrificed at either 16 or 64 h after AMPH. First, the rats were anesthetized with 80 mg/kg i.p. sodium pentobarbital and perfused with 50 ml saline followed by 250 ml of 4% formaldehyde in 0.1 M sodium phosphate buffer (pH 7.4). The brains were postfixed for at least 2 days in 4% formaldehyde, and then coronal sections 40 µm thick were cut and collected in 2% formaldehyde with 0.1 M phosphate (pH 7.4) and stored at 4 °C until processing. The two primary antisera against NPY were raised in either

rabbit (1:2000 dilution; Chemicon, Temecula, FL) or goat (1:100 dilution; Santa Cruz Biotech., CA) while the IGFBP-1 antisera was raised in rabbit (1:2000 dilution; Santa Cruz Biotech.). This immunoreaction signal was developed using the avidin and biotinylated horseradish peroxidase macromolecule complex (ABC, Vector Laboratories, Burlingame, CA), and visualized with 0.4 mg/ml of 3,3′-diaminobenzidine in 50 mM Tris buffer. GFAP-immunolabel was detected using a rabbit antiserum to GFAP (1:1000; Dako Corp., Carpinteria, CA) overnight at 4 °C, and then the ABC method and DAB as described above. Images were obtained using a SenSys cooled CCD digital camera mounted on a Nikon Eclipse E400 light/epifluorescent microscope and MetaView Imaging Software (Advanced Scientific, Inc., Meraux, LA).

RESULTS

Effects of AMPH on Body Temperature

The effects of the 2-day AMPH exposure on behavior and body temperature have been reported in detail elsewhere (Jakab and Bowyer, 2002). In summary, over 80% of the rats exposed to AMPH survived. Rats with peak body temperatures of 40.0 °C or above (<5% of the survivors) were removed from the studies. Overt behavioral seizure activity like that previously observed in mice and rats (Bowyer et al., 1998; Schmued and Bowyer, 1997) was not seen in the AMPH animals in the present study. There was no correlation between body temperature and neurodegeneration in either the parietal cortex or PLCo (Jakab and Bowyer, 2002).

Dopamine and TH Depletions and GFAP Elevations

The changes in dopamine, TH and GFAP levels after saline or AMPH can be seen in Fig. 1. Dopamine levels were dramatically depressed by more than 65% at both 64 h and 14 days post-AMPH. There was no significant difference in the magnitude of the depletions produced by AMPH at the two time points. Statistically, it was not clear whether differences in GFAP elevation in the striatum existed between 64 h and 14 days but TH was significantly decreased at 64 h compared to 14 days post-AMPH. A two-way ANOVA using day of sacrifice and dosing conditions as factors showed that dosing conditions (saline versus AMPH) significantly affected the levels of dopamine ($F(1,57) = 808.5$, $P < 0.001$) while time (64 h versus 14 days) of sacrifice did not ($F(1,57) = 3.39$, $P = 0.07$). There was significant interaction between the two factors ($F(1,57) = 6.95$, $P < 0.011$). With respect to GFAP, dosing conditions affected the levels of GFAP ($F(1,43) = 14.28$, $P < 0.001$) but neither the time of sacrifice ($F(1,43) = 0.43$, $P = 0.51$) nor the interaction between the two factors had a significant effect ($F(1,43) = 1.82$, $P = 0.128$). AMPH also significantly affected TH levels ($F(1,43) = 9.10$, $P = 0.004$) as did the time of sacrifice ($F(1,43) = 10.42$, $P < 0.002$) but the interaction between the two factors was not significant ($F(1,43) = 1.31$, $P = 0.239$). Neither the individual peak nor 2-day mean body temperatures during AMPH exposure correlated with the dopamine levels at either 64 h ($r = -0.30$, -0.05, respectively) or 14 days ($r = -0.29$, -0.14) after AMPH. Furthermore, there was no significant difference ($P = 0.655$ at 3 days and $P = 0.243$, at 14 days) between the magnitude of dopamine depletion in rats cooled either directly or indirectly with crushed ice (384 ± 32 ng/100 mg tissue, $n = 9$ at 3 days; 383 ± 37 ng/100 mg tissue, $n = 8$ at 14 days) with those not cooled with ice (404 ± 31 ng/100 mg tissue, $n = 10$ at 3 days; 452 ± 2 ng/100 mg tissue, $n = 9$ at 14 days). Finally, neither the peak nor mean body temperature over the dosing period affected TH ($r = 0.352$, -0.02, at 64 h; $r = 0.05$, 0.09, at 14 days) and GFAP levels ($r = -0.11$, -0.49, at 64 h; $r = -0.05$, -0.06, at 14 days).

cDNA Array Analysis

The differences in gene expression between four brain regions in the control animals have been described elsewhere (Delongchamp et al., 2003). Since the gene expression profiles significantly differed in all four of the brain regions, the data analysis to look for AMPH-induce changes in gene expression had to be determined on a region-by-region basis. No matter what method was used for data analysis, it was apparent that there were only a few short-term changes in gene expression induced by AMPH that were two-fold greater or lesser than control levels. In our analysis, statistical significance was determined for each gene by analysis of variance. The estimated effects were typically less than two-fold, and effects of this magnitude were not significant when data for each sacrifice time were analyzed separately. To garner more power the variances within sacrifice times were pooled to estimate the variance of treatment differences with more degrees of freedom. However, the false discovery rates estimated for these analyses were generally large

Table 1
Effects of 2-day AMPH on expression/mRNA levels of selected genes

Sacrifice time point after AMPH	Parietal cortex								
	Cyto. Ox. I	Hsp 90	Nur 77	NGFI-A	Arc	NPY-P	IGFBP-1	IGFBP-5	trkB
16 h	1.31	1.03	0.52	0.50	0.66	2.15	1.16	N.Q.	0.83
64 h	1.06	0.88	1.53	0.88	1.39	0.97	1.06	N.Q.	1.18
14 days	1.01	1.00	1.01	0.92	1.21	1.07	1.24	N.Q.	1.30
	PLCo								
	Cyto. Ox. I	Hsp 90	Nur 77	NGFI-A	Arc	NPY-P	IGFBP-1	IGFBP-5	trkB
16 h	1.21	1.10	0.85	1.01	0.78	1.03	1.80	1.49	1.10
64 h	1.18	1.12	1.62	1.36	1.28	1.53	2.14	1.32	1.37
14 days	1.15	0.95	0.84	1.07	0.98	0.89	1.11	1.36	1.05
	Striatum								
	Cyto. Ox. I	Hsp 90	Nur 77	NGFI-A	DA D1	DA D2	SP-P	NPY-P	trkB
16 h	0.97	1.02	N.Q.	0.93	0.99	0.96	1.12	1.11	0.96
64 h	0.88	0.84	N.Q.	0.96	0.97	0.99	0.97	1.04	1.06
14 days	0.87	1.15	N.Q.	1.30	0.99	0.90	0.90	0.95	0.95
	Substantia nigra								
	Cyto. Ox. I	Hsp 90	MIF	DAT	DA D1	DA D2	IGFBP-1	IGFBP-5	trkB
16 h	0.92	1.02	1.13	0.94	N.Q.	0.94	1.13	1.12	0.84
64 h	1.13	1.04	0.94	0.75	N.Q.	0.62	0.95	1.22	1.36
14 days	1.11	1.13	0.99	0.61	N.Q.	0.76	1.08	1.42	1.42

The fold changes in gene expression after AMPH are show relative to control at 16, 64 h and 14 days after AMPH.Abbreviations: Cyto. Ox. I, cytochrome oxidase I; DA D1, dopamine D1 receptor; DA D2, dopamine D2 receptor; DAT, plasma membrane associated dopamine transporter; Arc, activity-regulated cytoskeletal protein; Hsp 90, heat/shock-stress protein 84/90; IGFBP-1, IGFBP-5, insulin-like growth factor binding protein 1 and 5 precursor; MIF, macrophage migration inhibitory factor; NGFI-A, nerve growth factor-induced protein I-A; NGFI-B or Nur 77 (early response protein), nerve growth factor-induced protein I-B; NPY-P, neuropeptide Y precursor protein; SP-P, Substance P precursor protein; trkB, tyrosine receptor kinase B. N.Q.: levels so low that expression not quantified.

(25–75%) making it difficult to determine which genes had truly significantly different expression after AMPH. We chose genes for further analysis that were significantly affected by AMPH exposure at the 0.05 level in the PLCo and parietal cortex, which also had relatively large (>1.2- to 2-fold) changes in expression.

In Table 1, the expression levels of several selected genes are shown for the various brain regions and time points. They were selected because they are specific for dopaminergic cells, specific for dopamine innervation, reported to change during METH exposure by other investigators or appeared to have increased or decreased approximately two-fold from our cDNA array analysis. Interestingly, there were only a few genes that were found to significantly change expression in both the PLCo and parietal cortex at the same sacrifice time point. Annexin V (GB#M21730) was the only gene that increased expression (1.4-fold) 14 days after AMPH in both the PLCo and parietal cortex. However, there were eight genes that significantly change expression in both regions at 64 h after AMPH. Among these are glutathione synthase and *S*-transferase (GB#L38615 and GB#X02904) and nicotinic acetylcholine receptor 4 subunit a (GB#L31620), which decreased to 0.7- to 0.8-fold and interleukin-7 (GB#AF010464), NGFI-B (which decreased at 16 h after AMPH) and proteosome alpha type 3 (GB#M58593) which increased. These changes may be of relevance to the neurotoxic events.

cDNA Array Results and RT–PCR and Immunohistological Verification in the Parietal Cortex

With regard to the short-term changes in gene expression in the two-fold range, in the parietal cortex, cDNA array analysis indicated that neuropeptide Y precursor protein (NPY-P) mRNA was increased two-fold while nerve growth factor protein IA (NGFI-A; a.k.a. early growth response protein 1, EGR-1) and nerve growth factor protein IB (NGF-IB, a.k.a. Nur 77) mRNAs decreased 50% and Arc mRNA decreased 40% at the 16 h time point (Fig. 2, Table 1). Nur 77 (Ngfi-B) expression was slightly elevated at the 64 h

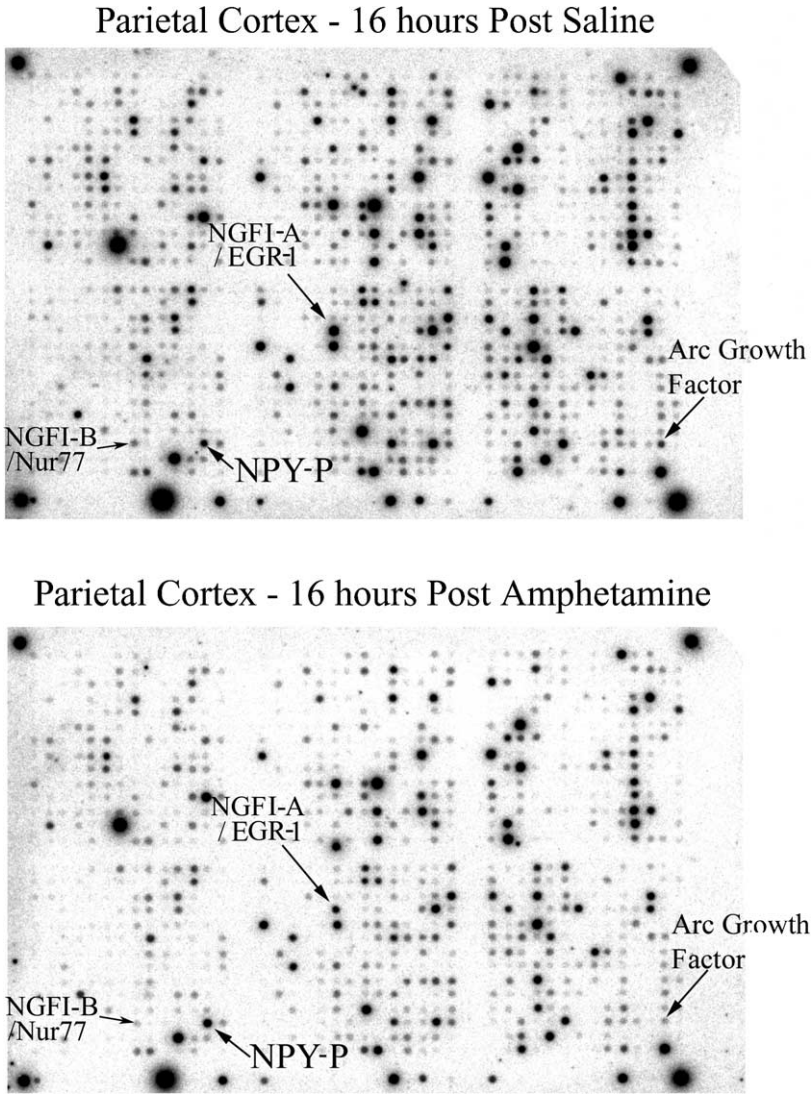

Fig. 2. Arrays hybridized with cDNA target generated from parietal cortex RNA obtained 16 h post-dosing from either saline or AMPH-treated animals. Phosphor images of arrays hybridized with ^{32}P-dATP-labeled cDNA target made from total RNA obtained from parietal cortex 16 h post either 2-day saline (top) or 2-day AMPH (bottom) are shown. Three genes showed a significant trend in differential expression when multiple pairs of control and AMPH from this same time point and brain region were analyzed. In AMPH-treated animals, neuropeptide Y precursor (NPY-P) mRNA increased two-fold while, neuronal growth factor-induced receptor protein A mRNA (EGR-1 or NGFI-A) and neuronal growth factor-induced receptor protein B (Nur 77 or NGF-IB) mRNA decreased more than 50%. Arc growth factor mRNA also indicated a somewhat downward trend.

time point in the parietal cortex. RT–PCR also showed that Npy-P expression was increased more than two-fold and Ngfi-a expression was decreased more than 50% in the parietal cortex at 16 h (Table 2). As well RT–PCR indicated that GFAP mRNA (not present on this cDNA array) might be slightly elevated at 16 and 64 h.

Histological evaluation of the parietal cortex after AMPH does not show any overt changes in the NPY-P derived protein level of the neurotransmitter NPY (Fig. 3). Overt morphological signs of damage were not detected in cortical NPY-immunoreactive neurons, but swollen, irregularly twisted NPY-immunoreactive axons were encountered in layers II–III, an increase in GFAP (gene not present on the cDNA array) mRNA from RT–PCR analysis (Table 2). Array analysis indicated that insulin-like growth factor binding protein 1 (IGFBP-1) mRNA was not affected in the parietal cortex (Table 1).

cDNA Array Results and RT–PCR and Immunohistological Verification in the PLCo

In contrast to the parietal cortex, in the PLCo a two-fold increase in IGFBP-1 mRNA was seen at 16 and 64 h with either cDNA array or RT–PCR analysis

Table 2
Effects of 2-day AMPH on mRNA levels of selected genes evaluated by RT–PCR

mRNA species	Number of cycles to optical threshold (C_t)		Expression relative to GAPDH (ΔC_t)		Effect of AMPH on expression relative to saline
	Saline	AMPH	Saline	AMPH	
Parietal cortex at 16 h post-AMPH					
28S	10.2 ± 0.2	10.3 ± 0.1	−7.2	−7.1	+0.1
GAPDH	17.4 ± 0.6	17.4 ± 0.5	–	–	–
NPY-P	24.3 ± 0.5	23.0 ± 0.5 a	+6.9	+5.6	−1.3
EGR-1 (NGFI-A)	20.1 ± 0.7	21.4 ± 0.6 b	+2.7	+4.0	+1.3
GFAP[a]	20.4 ± 0.2	19.6 ± 0.7	+3.0	+2.2	−0.8
PLCo at 16 and 64 h post-AMPH					
28S	10.0 ± 0.2	10.1 ± 0.2	−7.5	−7.5	0.0
GAPDH	17.5 ± 0.4	17.6 ± 0.8	–	–	–
NPY-P	25.3 ± 0.6	24.9 ± 0.8	+7.8	+7.3	−0.5
EGR-1 (NGFI-A)	23.2 ± 0.4	22.5 ± 0.8	+5.7	+4.9	−0.8
IGFBP-1	31.8 ± 0.4	31.0 ± 0.4	+14.3	+13.4	−0.9
GFAP[a]	19.4 ± 0.3	19.1 ± 0.7	+1.9	+1.5	−0.4
Substantia nigra at 14 days post-AMPH					
28S	10.4 ± 0.2	10.6 ± 0.5	−7.5	−7.0	+0.5
GAPDH	17.9 ± 0.2	17.6 ± 0.5	–	–	–
NPY-P	28.4 ± 0.2	28.0 ± 0.6	+10.5	+10.4	−0.1
EGR-1 (NGFI-A)	26.0 ± 0.6	25.4 ± 0.8	+8.2	+7.8	−0.4
DAT	20.4 ± 0.5	21.0 ± 0.3	+2.5	+3.4	+0.9
TH	19.6 ± 0.3	19.7 ± 0.5	+1.7	+2.1	−0.4
Striatum at 16 and 64 h post-AMPH					
28S	10.4 ± 0.9	10.9 ± 0.4	−7.5	−7.3	+0.2
GAPDH	17.9 ± 0.4	18.2 ± 0.4	–	–	–
GFAP[a]	19.5 ± 0.4	19.0 ± 0.6	+1.6	+0.8	−0.8

[a] Not present on array.

Mean ± S.E.M. shown in the table were generated from the RT–PCR values determine for the RNA aliquots (for each aliquot several RT–PCR runs were averaged determine its value) used at each time point. For each time point and brain region there were between three and five aliquots of control RNA and four and six aliquots of RNA derived from AMPH-treated rats.

(Tables 1 and 2). IGFBP-1 labeled many neurons and axon-like processes in pyramidal and non-pyramidal neuron types throughout the brain including the PLCo. In the controls, IGFBP-1 staining/immunoreactivity intensity was moderate and the staining pattern was mainly restricted to perikarya (Fig. 4). However, in the treated rats, IGFBP-1 immunostaining was markedly more intense and strongly labeled long dendritic processes. NPY-P mRNA was not elevated at 16 h in the PLCo but levels appeared to be somewhat elevated at 64 h from array as well as RT–PCR data (Table 2). A slight increase in the GFAP mRNA expression in the PLCo within the first 64 h after AMPH exposure was seen with RT–PCR (Table 2).

cDNA Array Results and RT–PCR Verification in the Striatum and Substantia Nigra

In the striatum, there were no two-fold changes in the expression in any of the genes monitored at any of the time points (Table 1). There appears to be about a 1.5-fold increase in GFAP mRNA and protein levels in the striatum (Fig. 1, Table 2). Changes in the substantia nigra were not observed at 16 h after AMPH. However, at 64 h and at 14 days the expression of both Dat and dopamine D2 receptors appeared to be somewhat decreased according to both cDNA array and RT–PCR analysis (Tables 1 and 2).

The Effects of AMPH-Induced Hemorrhage on the Gene Expression in the Parietal Cortex

When hemorrhagic stroke occurred during AMPH exposure gene expression was markedly altered. In one of the rats sacrificed at 14 days post-AMPH signs of a unilateral hemorrhage in one hemisphere over the parietal cortex was noted during dissection. Total RNA from this hemisphere rat was isolated separately, and cDNA array analysis was subsequently performed on this RNA (Fig. 5). There were marked (three-fold or

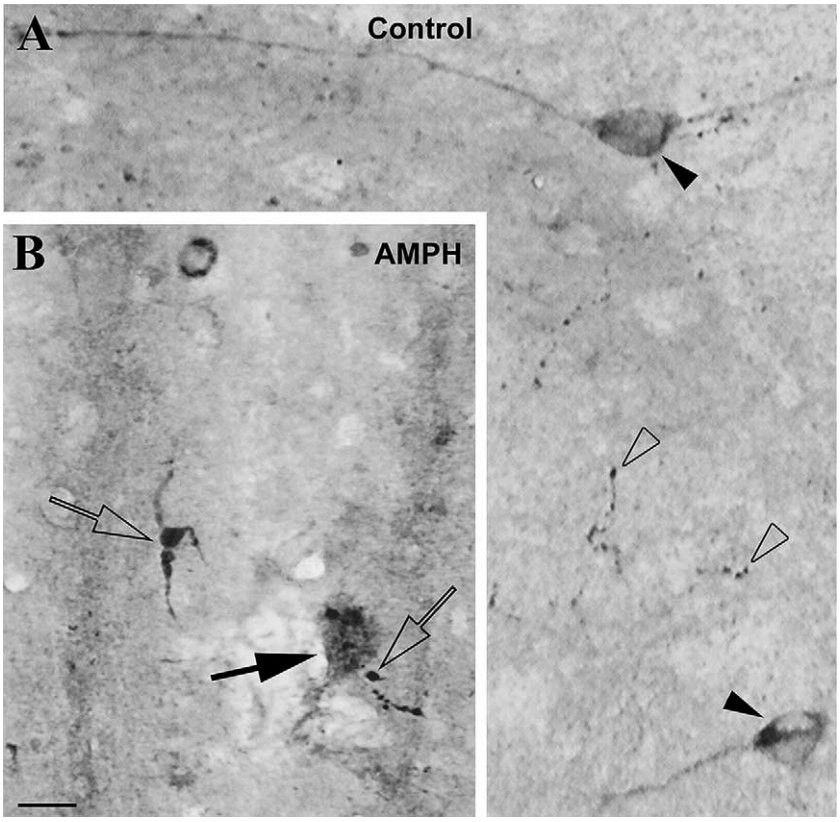

Fig. 3. Histological localization of NPY immunoreactivity within the parietal cortex and striatum at 16 h after AMPH exposure. A comparison of the NPY immunoreactivity around layer IV of barrels within the somatosensory parietal cortex is seen at 16 h after the end of either saline (plate A) or AMPH (plate B) treatment. Open arrows indicate fibers while solid arrows locate the position of cell bodies. Some swollen NPY fibers and abnormal cytoplasmic NPY staining granules in the cells of AMPH-treated animals indicate the possibility of damage within some NPY neurons. However, the overall intensity of the NPY staining in the somatosensory parietal cortex of control and AMPH-treated animals was not appreciably different.

more) changes in the expression of over 30 genes in the parietal cortex of this animal with almost 50% of the changes occurring in cyclins, neurotrophic/growth factors and neurotransmitter receptors. Marked increases were seen in the expression of genes that normally occur at extremely low levels in cortex such as interleukins, interleukin receptors and Hsp 70 inducible.

DISCUSSION

There are implications for the short-term (16 and 64 h) changes in NPY-P/NPY and IGFBP-1 levels in the neurotoxic events that occur in the cortex after 2-day AMPH exposure. The NPY increases in the parietal cortex are due in part to dopamine's general stimulating effect on NPY-P gene expression (Lindefors et al., 1990). Increased NPY release may be dampening the susceptibility of pyramidal neurons in layer III as well as parvalbumin containing interneurons in layer IV to excitotoxic damage during AMPH exposure (Jakab and Bowyer, 2002). This hyper-stimulation may lead to the degeneration of NPY interneurons in layer II under some circumstances (Fig. 4; Jakab and Bowyer, unpublished data). The protective effects of NPY have been proposed for other types of neurotoxic insults (Cheung and Cechetto, 1995; Kopp et al., 1999). Acute exposure to METH has been observed to decrease the levels of NPY protein in the extrapyramidal and limbic systems of the rat (Westwood and Hanson, 1999), and we did not observe increased NPY immunoreactivity in the parietal cortex even though NPY-P mRNA increased. However, a significant increase in the release and degradation of NPY would explain why increased neuronal NPY levels did not occur. With respect to IGFBP-1, its increased expression in AMPH-sensitive cortical regions could represent an important step in the neuroprotective/regenerative processes in the PLCo.

The differences we observed in the AMPH-induced the short-term changes in expression of NPY-P and IGFBP-1 in the parietal cortex compared to the PLCo

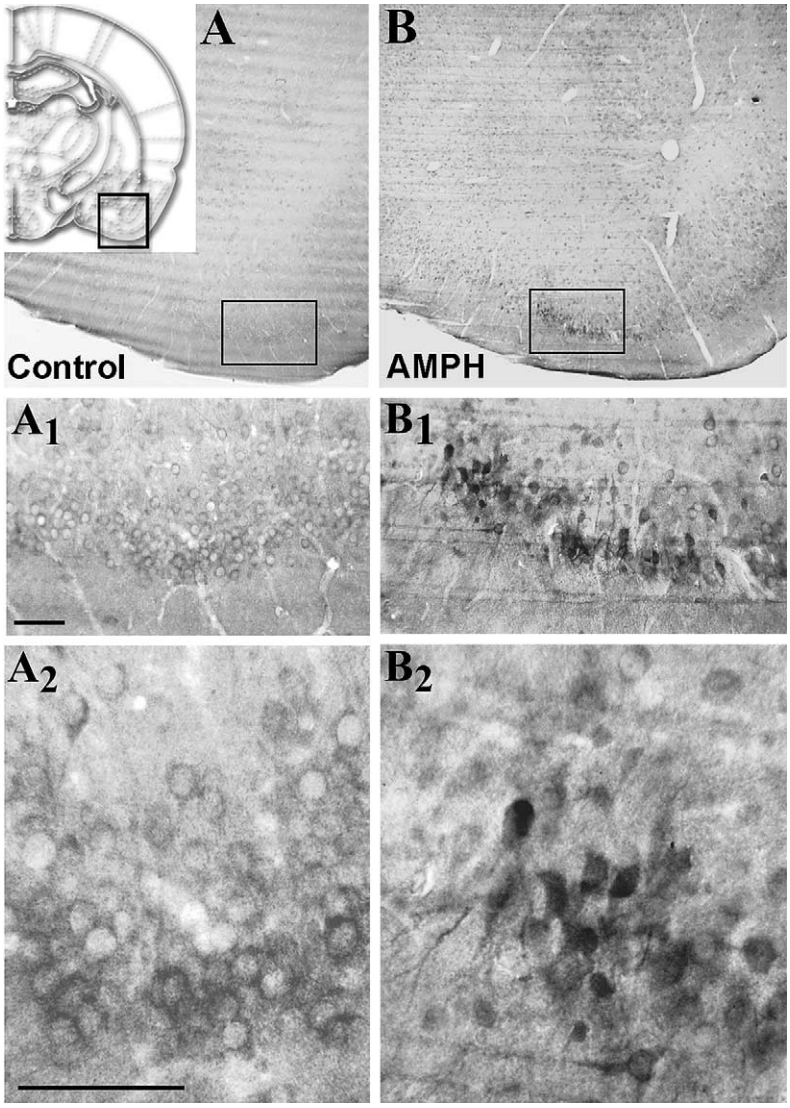

Fig. 4. Histological localization of IGFBP-1 immunoreactivity within the PLCo at 16 h after AMPH exposure. A comparison of the IGFBP-1 immunoreactivity in the PLCo in control (plates A–A_2) and AMPH-treated (plates B–B_2) animals at 64 h after dosing. In the AMPH-treated animals the immunoreactivity of IGFBP-1 is appreciably higher in some of the cell bodies, and more extensively labels dendritic processes than in the control brain.

would not have been readily predicted. These differences may be in part due to differences in the distribution of NPY and IGFBP-1 between the parietal cortex and the PLCo. NPY is present in layer II of the parietal cortex (Wang et al., 2002) but in lower abundance in the PLCo. In contrast, IGFBP-1 immunoreactivity was present in higher levels in layer II of the PLCo than in neighboring layers but was the least abundant in layer IV of the parietal cortex compared to neighboring supra- and infra-granular layers. Therefore, multifold changes in the levels of IGFBP-1 mRNA in layer IV of the parietal cortex might not significantly increase the overall levels of the message in the entire parietal cortex because the levels were so much higher in layers III and V. A similar effect could be occurring in the PLCo with respect to NPY levels since they are much lower in layer II of the PLCo. An alternative explanation is that the neurodegenerative and/or repair/protective processes differ in these regions.

The reasons behind the down-regulation of NGFI-A (a.k.a. EGR-1, *zif*268) and NGFI-B (a.k.a. Nur 77) and ARC mRNA levels at 16 h occurring only in the parietal cortex but not in the PLCo are not known. NGFI-A, NGFI-B and ARC mRNA are known to be up regulated in rodents within several hours after AMPH exposure (Wang et al., 1994; Backman and Morales, 2002; Kodama et al., 1998). The decrease in these three mRNA levels 16 h after the 2-day AMPH exposure may occur either to facilitate the return of elevated protein levels of this gene that occurred during AMPH

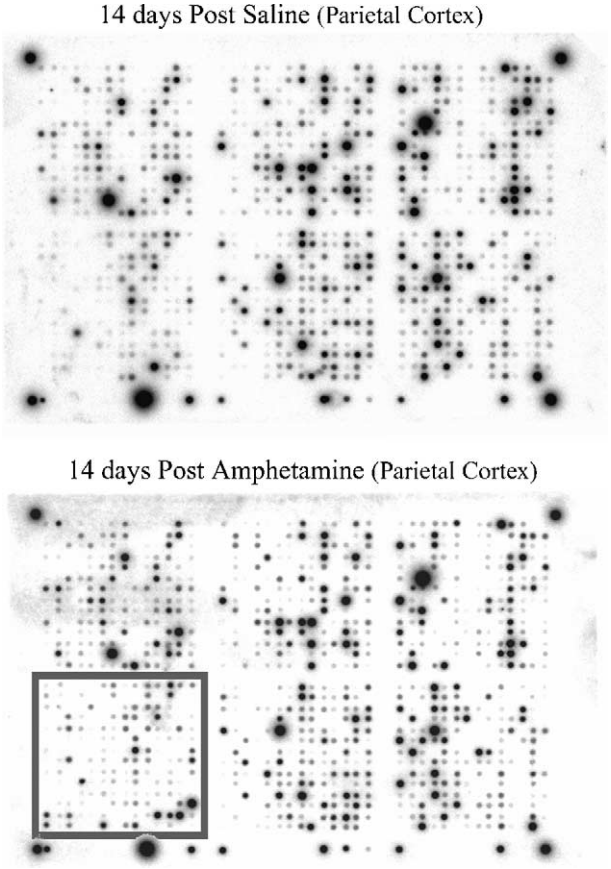

Fig. 5. Stroke produced from AMPH exposure results in pronounced changes in the expression of many genes. The changes in gene expression in the parietal cortex of AMPH-treated animal that suffered a unilateral hemorrhage were prominent at 14 days after dosing. Over 30 genes had significantly altered expression three-fold or more above control many of them within the rectangle in the lower left corner of the array from the parietal cortex from stroke hemisphere. Most of the changes in gene expression were from trophic/growth-related factors, stress protein and immune response genes such as the interleukins.

exposure back to ''normal'' or as some type of response to toxic insult within the region. Why this does not also occur in the PLCo is not clear. Also, it is not known why NGFI-B appears to increase 1.5-fold in both cortical regions at 64 h after AMPH.

Although there were several two-fold short-term changes in gene expression, long-term changes above 1.5-fold were not observed in the parietal cortex and PLCo. The only gene to significantly change expression in both cortical regions 14 days after AMPH was annexin V. This may be an indicator that neuronal degeneration has taken place in these regions since annexin A5 has been reported to identify apoptotic cells (Reutelingsperger et al., 2002). We originally hypothesized that the damage produced in the parietal cortex and PLCo by the 2-day AMPH exposure would likely produce long-term, as well as short-term, changes in gene expression in these regions. With either acute (Bowyer et al., 1998; Eisch and Marshall, 1998; Eisch et al., 1998) or 2-day AMPH exposure (Jakab and Bowyer, 2002) the axonal damage and astrocytosis extends to the layers surrounding cortical layer II of the PLCo and III and IV of the somatosensory parietal cortex where neurodegeneration occurs. One might assume that all barrel fields in the somatosensory region receive excessive excitatory input during the 2 days of dosing, and that this could also lead to short- and long-term changes in gene expression. If these cortical-wide changes in gene expression occur they are in the 1. 5-fold or less range.

More prominent changes in gene expression after 2-day AMPH exposure may not have occurred as a result of two factors. These are the (1) ''dilution'' factors with regard to total RNA obtained by regional brain dissection and (2) damage and hyper-stimulation of one particular layer of the cortex does not necessarily entail changes in the gene expression of the other layers within that brain region. In regards to ''dilution'' factors, only specific regions within the neocortex (parietal cortex, layer IV) and the paleocortex (PLCo and adjacent piriform cortex, layer II) are notably damaged, and the damage within these layers is highly variable between barrels or sub-areas. Thus, the neuronal degeneration occurs only within 1–10% of the total volume of the cortex dissected for RNA isolation. If gene expression is minimally affected in the cortical regions where no neurodegeneration occurs, then a 10- to 100-fold dilution factor occurs, and obscures the ability to see the gene expression changes within the damaged regions.

The effects of ''dilution'' have also interfered with the evaluation of changes in NMDA receptor protein (changes in the NMDA receptor binding) in whole region homogenates of parietal cortex after METH (Bowyer et al., 1994). However, NMDA receptor changes could be detected after METH within layers III and IV using more discrete histological methods detecting NMDA receptors of the parietal cortex (Eisch et al., 1996). The phenomenon of ''dilution'' factors obscuring changes in gene expression within a discrete region of the cortex has been previously considered in interpreting the results of cDNA analysis of gene expression (Mirnics, 2001; Mirnics et al., 2001). Nonetheless, there appear to be some short-term and long-term changes in the 1.2- to 1.5-fold range in both the PLCo and parietal cortex that are significant and potentially influenced by neurotoxicity. If these are the result of larger changes within discrete populations of neurons in the regions, then studies using either

immunohistochemical techniques or laser capture microscopy should more readily verify these changes.

Previous METH and AMPH studies in mice and rats have observed more two-fold or greater changes in gene expression than did our present study (Cadet et al., 2001; Jayanthi et al., 2002; Xie et al., 2002; Sokolov et al., 2003). These differences between studies involving AMPH- and METH-induced changes in gene expression are due, in part, to factors such as (1) hyperthermia, (2) seizure activity, (3) dosing paradigms and (4) shorter time intervals between the end of exposure and sacrifice. In all the previous studies significant hyperthermia would be expected to occur during drug exposure, and in the mice studies (Cadet et al., 2001; Jayanthi et al., 2002; Xie et al., 2002) both prominent and extended hyperthermia and seizure-like activity would occur (Miller and O'Callaghan, 1994; O'Callaghan and Miller, 1994; Schmued and Bowyer, 1997; Xie et al., 2002; Bowyer and Ali, unpublished data). Acute exposure to moderate and high doses of AMPH and METH, that produce seizure activity and significant hyperthermia, are known to induce the expression of heat-shock/stress proteins and early/immediate genes (O'Dell and Marshall, 2002; Wang et al., 1994; Nguyen et al., 1992; Goto et al., 1993; Nowak, 1988). However, seizure activity and hyperthermia alone, in the absence of AMPH or METH, produce many of these changes in early-immediate gene expression (Kiessling and Gass, 1993), as well as neurotrophins (Gall, 1993) and even reference genes (Chen et al., 2001).

The dosing paradigm used in the present studies did not produce hyperthermia and overt signs of seizure-activity during AMPH exposure (Jakab and Bowyer, 2002), and resulted in only a few selected two-fold changes in gene expression levels at 16 and 64 h after dosing in the damaged cortical regions. Nonetheless, neurodegeneration produced by the 2-day AMPH in the PLCo and parietal cortex was as extensive as that reported in rodents exposed to METH or AMPH when hyperthermia and seizures occurred (Bowyer et al., 1998, 2001; Schmued and Bowyer, 1997). The neurotoxic effects produced by the 2-day AMPH exposure may be similar to the milder forms of neurotoxicity observed in some human studies (Wilson et al., 1996) and fewer changes in gene expression might be expected. On the other hand, the acute high-dose exposure neurotoxicity seen in rodents may model the types of neurotoxicity sometimes produced in humans with life-threatening exposures (Bowyer and Holson, 1995; Davidson et al., 2001; Deng et al., 2001).

Non-neurotoxic dosing regimens of cocaine have been previously shown to produce either long-term decreases (Letchworth et al., 1999) or in some instances increases (Lu and Wolf, 1997) in DAT mRNA in the substantia nigra. Furthermore, neurotoxic doses of METH that damage terminals but do not cause degeneration of dopaminergic neuron greatly reduce DAT levels (Wagner et al., 1980). Thus, it is not entirely surprising that the expression of Dat was also down-regulated by the 2-day AMPH exposure in the present studies, even though there were no histological signs of gliosis or neurodegeneration in the substantia nigra (Jakab and Bowyer, 2002). Chronic exposure to cocaine, AMPH and METH are known to cause long-term changes in gene expression in other areas of the brain such as ventral tegmentum, frontal cortex and nucleus accumbens (Freeman et al., 2001a,b; Koob and Nestler, 1997; Miki, 2001; Nestler and Aghajanian, 1997). Therefore, with respect to stimulants such as AMPH and METH, chronic exposures may be more likely than neurotoxic exposures to result in long-term changes in gene expression. As well, the regions in which these changes occur may not be those most susceptible to AMPH- or METH-induced neurotoxicity.

In conclusion, the 2-day AMPH dosing paradigm, produced neurotoxicity in specific cortical regions and some selective short-term two-fold changes in the gene expression in the parietal cortex (Npyp, NgfI-A) and PLCo (Igfbp-1), that are likely related to neurotoxicity, without inducing hyperthermia and seizures. Long- and short-term changes in expression less than 1.5-fold were more numerous within these cortical regions; however, these lesser changes may be of importance and related to neurotoxicity. Greater fold-changes in gene expression may not have been seen because of "dilution factors" that resulted from using RNA derived from the entire brain regions where neurotoxicity occurs. Further studies are necessary to determine if more prominent changes in gene expression occur within discrete cortical layers and sub-populations of neurons within these regions. Finally, DAT and dopamine D_2 receptors are down-regulated 14 days after AMPH exposure in the substantia nigra, which is an area spared from neurodegeneration and astrocytosis. Therefore, long-term changes in gene expression may not necessarily coincide with the areas where overt signs of neurotoxicity occur.

ACKNOWLEDGEMENTS

The authors acknowledge the efforts of Xiaoxi Cao and Steven Harris in Biometry at NCTR for their help

in data processing and the statistical analysis of the cDNA array work.

REFERENCES

Backman C, Morales M. Acute methamphetamine administration upregulates NGFI-B mRNA expression in the striatum. Synapse 2002;44:158–65.

Bates S, Read SJ, Harrison DC, Topp S, Morrow R, Gale D, Murdock P, Barone FC, Parsons AA, Gloger IS. Characterization of gene expression changes following permanent MCAO in the rat using subtractive hybridization. Mol Brain Res 2001;293: 70–80.

Benjamini Y, Hochberg Y. On the adaptive control of the false discovery rate in multiple testing with independent statistics. J Educ Behav Stat 2000;25:60–83.

Bowyer JF. Neuronal degeneration in the limbic system of weanling rats exposed to saline, hyperthermia or D-amphetamine. Brain Res 2000;885:166–71.

Bowyer JF, Holson RR. Methamphetamine and amphetamine neurotoxicity: characteristics, interactions with body temperature and possible mechanisms. In: Chang LW, Dyer RS, editors. Handbook of neurotoxicology, vol. II. New York, Basel, Hong Kong: Marcel Dekker Inc.; 1995. p. 845–70.

Bowyer JF, Tank AW, Newport GD, Slikker Jr, W, Ali SF, Holson RR. The influence of environmental temperature on the transient effects of methamphetamine on dopamine release in rat striatum. J Pharmacol Exp Ther 1992;260:817–24.

Bowyer JF, Davies DL, Schmued L, Broening HW, Newport GD, Slikker Jr, W, Holson RR. Further studies of the role of hyperthermia in methamphetamine neurotoxicity. J Pharmacol Exp Ther 1994;268:1571–80.

Bowyer JF, Peterson SL, Rountree RL, Tor-Agbidye J, Wang GJ. Neuronal degeneration in rat forebrain resulting from D-amphetamine-induced convulsions is dependent on seizure severity and age. Brain Res 1998;809:77–90.

Bowyer JF, Holson RR, Miller DB, O'Callaghan JP. Phenobarbital and dizocilpine can block methamphetamine-induced neurotoxicity in mice by mechanisms that are independent of thermoregulation. Brain Res 2001;919:179–83.

Cadet JL, Jayanthi S, McCoy MT, Vawter M, Ladenheim B. Temporal profiling of methamphetamine-induced changes in gene expression in the mouse brain: evidence from cDNA array. Synapse 2001;41:40–8.

Chen J, Sochivko D, Beck H, Marechal D, Wiestler OD, Becker AJ. Activity-induced expression of common reference genes in individual CNS neurons. Lab Invest 2001;81:913–6.

Cheung RT, Cechetto DF. Neuropeptide changes following excitotoxic lesion of the insular cortex in rats. J Comp Neurol 1995;362:535–50.

Chomczynski P. A reagent for the single-step simultaneous isolation of RNA, DNA and proteins from cell and tissue samples. Biotechniques 1993;15:532–7.

Chomczynski P. Modification of the TRI reagent procedure for isolation of RNA from polysaccharide- and proteoglycan-rich sources. Biotechniques 1995;19:532–7.

Davidson C, Gow AJ, Lee TH, Ellinwood EH. Methamphetamine neurotoxicity: necrotic and apoptotic mechanisms and relevance to human abuse and treatment. Brain Res 2001;36:1–22.

Delongchamp RR, Harris AJ, Bowyer JF. A statistical approach in using cDNA array analysis to find modest, 2-fold or less, changes in gene expression in several brain regions after neurotoxic insult. Ann NY Acad Sci 2003;993:363–76.

Deng X, Wang Y, Chou J, Cadet JL. Methamphetamine causes widespread apoptosis in the mouse brain: evidence from using an improved TUNEL histochemical method. Brain Res 2001; 93:64–9.

Eisch AJ, Marshall JF. Methamphetamine neurotoxicity: dissociation of striatal dopamine terminal damage from parietal cortical cell body injury. Synapse 1998;30:433–45.

Eisch AJ, O'Dell SJ, Marshall JF. Striatal and cortical NMDA receptors are altered by a neurotoxic regimen of methamphetamine. Synapse 1996;22:217–25.

Eisch AJ, Schmued LC, Marshall JF. Characterizing cortical neuron injury with Flouro-Jade labeling after a neurotoxic regimen of methamphetamine. Synapse 1998;30:329–33.

Ernst T, Chang L, Leonido-Yee M, Speck O. Evidence for long-term neurotoxicity associated with methamphetamine abuse. Neurology 2000;54:1344–9.

Freeman WM, Robertson DJ, Vrana KE. Fundamentals of DNA hybridization arrays for gene expression analysis. Biotechniques 2000;29:1042–6.

Freeman WM, Brebner K, Lynch WJ, Robertson DJ, Roberts DC, Vrana KE. Cocaine-responsive gene expression changes in rat hippocampus. Neurosciences 2001a;108:371–80.

Freeman WM, Nader MA, Nader SH, Robertson DJ, Gioia L, Mitchell SM, Daunais JB, Porrino LJ, Friedman DP, Vrana KE. Chronic cocaine-mediated changes in non-human primate nucleus accumbens gene expression. J Neurochem 2001b;77:542–9.

Gall CM. Seizure-induced changes in neurotrophin expression: implications for epilepsy. Exp Neurol 1993;124:150–66.

Goto S, Korematsu K, Oyama T, Yamada K, Hamada J, Inoue N, Nagahiro S, Ushio Y. Neuronal induction of 72-kDa heat shock protein following methamphetamine-induced hyperthermia in the mouse hippocampus. Brain Res 1993;626:351–6.

Jakab RL, Bowyer JF. Parvalbumin neuron circuits and microglia in three dopamine-poor cortical regions remain sensitive to amphetamine exposure in the absence of hyperthermia, seizure and stroke. Brain Res 2002;958:52–69.

Jayanthi S, Deng X, Bordelon M, McCoy MT, Cadet JL. Methamphetamine causes differential regulation of pro-death and anti-death Bcl-2 genes in the mouse neocortex. FASEB J 2002;15:1745–52.

Kiessling M, Gass P. Immediate early gene expression in experimental epilepsy. Brain Pathol 1993;3:381–93.

Kodama M, Akiyama K, Ujike H, Shimizu Y, Tanaka Y, Kuroda S. A robust increase in expression of Arc gene, an effector immediate early gene, in the rat brain after acute and chronic methamphetamine administration. Brain Res 1998;796:273–83.

Koob GF, Nestler EJ. The neurobiology of drug addiction. J Neuropsychiatry Clin Neurosci 1997;9:482–97.

Kopp J, Nanobashvili A, Kokaia Z, Lindvall O, Hokfelt T. Differential regulation of mRNAs for neuropeptide Y and its receptor subtypes in widespread areas of the rat limbic system during kindling epileptogenesis. Brain Res Mol Brain Res 1999;72:17–29.

Lee MLT, Kuo FC, Whitmore GA, Sklar J. Importance of replication in microarray gene expression studies: statistical methods and evidence from repetitive cDNA hybridizations. PNAS 2000;97:9834–9.

Letchworth SR, Sexton T, Childers SR, Vrana KE, Vaughan RA, Davies HM, Porrino LJ. Regulation of rat dopamine transporter mRNA and protein by chronic cocaine administration. J Neurochem 1999;73:1982–9.

Lindefors N, Brene S, Herrera-Marschitz M, Persson H. Regulation of neuropeptide Y gene expression in rat brain. Ann NY Acad Sci 1990;611:175–85.

Lu W, Wolf WE. Expression of dopamine transporter and vesicular monoamine transporter 2 mRNAs in rat midbrain after repeated amphetamine administration. Mol Brain Res 1997;49: 137–48.

McCann UD, Wong DF, Yokoi F, Villemange V, Dannals RF, Ricaurte GA. Reduced striatal dopamine transporter density in abstinent methamphetamine and methcathione users: evidence from positron emission tomography studies with [^{11}C]WIN-35,428. J Neurosci 1998;18:8417–22.

Miki N. Gene expression by addictive drugs and drug dependence. Nihon Shinkei seishin Yakurigaku Zasshi 2001;2: 127–31.

Miller DB, O'Callaghan JP. Environment-, drug- and stress-induced alterations in body temperature affect the neurotoxicity of substituted amphetamines in the C57BL/6J mouse. J Pharmacol Exp Ther 1994;270:752–60.

Mirnics K. Microarrays in brain research: the good, the bad and the ugly. Nature Rev Neurosci 2001;2:444–7.

Mirnics K, Middleton FA, Marquez A, Lewis DA, Levitt P. Molecular characterization of schizophrenia viewed by microarray analysis of gene expression in prefrontal cortex. Neuron 2001;28:53–67.

Nestler EJ, Aghajanian GK. Molecular and cellular basis of addiction. Science 1997;278:58–63.

Nguyen TV, Kosofsky BE, Birnbaum R, Cohen BM, Hyman SE. Differential expression of c-fos and zif/268 in rat striatum after haloperidol, clozapine, and amphetamine. Proc Natl Acad Sci USA 1992;89:4270–4.

Nowak TS. Effects of amphetamine on protein synthesis and energy metabolism in mouse brain: role of drug-induced hyperthermia. J Neurochem 1988;50:285–94.

O'Callaghan JP. Quantification of glial fibrillary acidic protein: comparison of slot-immunobinding assays with a novel sandwich ELISA. Neurotoxicol Teratol 1991;13:275–81.

O'Callaghan JP. Measurement of glial fibrillary acidic protein. In: Costa LG, editor. Current protocols in toxicology. New York: Wiley; 2002. p. 12.81.1–.2.

O'Callaghan JP, Miller DB. Neurotoxicity profiles of substituted amphetamines in the C57BL/6J mouse. J Pharmacol Exp Ther 1994;270:741–51.

O'Callaghan JP, Miller DB. Neurotoxic effects of substituted amphetamines in rats and mice. In: Massaro EJ, editor. Handbook of neurotoxicology, vol. 2. Totowa, NJ: Humana Press Inc.; 2001. p. 269–301.

O'Dell SJ, Marshall JF. Effects of vibrissae removal on methamphetamine-induced damage to rat somatosensory cortical neurons. Synapse 2002;43:122–30.

Paxinos G, Watson C. The rat brain in stereotaxic coordinatesm, vol. 2. San Diego, CA: Academic Press; 1995.

Reinhard Jr, JF, O'Callaghan JP. Measurement of tyrosine hydroxylase apoenzyme protein by enzyme-linked immunosorbent assay (ELISA): effects of 1-methyl-4-phenyl-1,2,3,6-tetrahydropyridine (MPTP) on striatal tyrosine hydroxylase activity and content. Anal Biochem 1991;196:296–301.

Reutelingsperger CP, Dumont E, Thimister PW, van Genderen H, Kenis H, van de Eijnde S, Heidendal G, Hofstra L. Visualization of cell death in vivo with annexin A5 imaging protocol. J Immunol Meth 2002;265:123–32.

Schmued LC, Bowyer JF. Methamphetamine exposure can produce neuronal degeneration in mouse hippocampal remnants. Brain Res 1997;759:135–40.

Schweder T, Spjotvoll E. Plots of *P*-values to evaluate many tests simultaneously. Biometrika 1982;69:493–502.

Seiden LS, Sabol KE. Neurotoxicity of methamphetamine-related drugs and cocaine. In: Chang LW, Dyer RS, editors. Handbook of neurotoxicology, vol. 2. New York, Basel, Hong Kong: Marcel Dekker, Inc.; 1995. p. 824–44.

Smith PK, Krohn RI, Hermanson GT, Mallia AK, Gartner FH, Provenzano MD, Fujimoto EK, Goeke NM, Olson BJ, Klenk DC. Measurement of protein using bicinchoninic acid. Anal Biochem 1985;150:76–85.

Sokolov BP, Polesskaya OO, Uhl GR. Mouse brain gene expression changes after acute and chronic amphetamine. J Neurochem 2003;84:244–52.

Sonsalla PK, Nicklas WJ, Heikkila RE. Role for excitatory amino acids in methamphetamine-induced nigrostriatal dopaminergic toxicity. Science 1989;243:398–400.

Stephans SE, Yamamoto BK. Methamphetamine-induced neurotoxicity: roles for glutamate and dopamine efflux. Synapse 1994; 17:203–9.

Storey JA. A direct approach to false discovery rates. J R Stat Soc B 2002;64:479–98.

Tang Y, Lu A, Aronow BJ, Sharp FR. Blood genomic responses differ after stroke, seizures, hypoglycemia and hypoxia: blood genomic fingerprints of disease. Ann Neurol 2001;50: 699–707.

Volkow ND, Chang L, Wang GJ, Fowler JS, Leonido-Yee M, Franceschi D, Sedler MJ, Gatley SJ, Hitzemann R, Ding YS, Logan J, Wong C, Miller EN. Association of dopamine transporter reduction with psychomotor impairment in methamphetamine abusers. Am J Psychiatry 2001a;158: 377–82.

Volkow ND, Chang L, Wang GJ, Fowler JS, Leonido-Yee M, Franceschi D, Sedler MJ, Gatley SJ, Hitzemann R, Ding YS, Wong C, Logan J. Higher cortical and lower subcortical metabolism in detoxified methamphetamine abusers. Am J Psychiatry 2001b;158:383–9.

Wagner GC, Ricaurte GA, Johanson CE, Schuster CR, Seiden LS. Amphetamine induces depletion of dopamine and loss of dopamine uptake sites in the caudate. Neurology 1980;30: 547–50.

Wang JQ, Daunias JB, McGinty JF. NMDA receptors mediate amphetamine-induced upregulation of zif/268 and preprodynorphin mRNA expression in rat striatum. Synapse 1994;18: 343–53.

Wang Y, Gupta A, Toledo-Rodriguez M, Wu CZ, Markram H. Anatomical, physiological, molecular and circuit properties of nest basket cells in the developing somatosensory cortex. Cereb Cortex 2002;12:395–410.

Westwood WC, Hanson GR. Effects of stimulants of abuse on the extrapyramidal and limbic neuropeptide Y systems. J Pharmacol Exp Ther 1999;288:1160–8.

Westman J, Sharma HS. Heat shock protein response in the central nervous system following hyperthermia. Prog Brain Res 1998; 115:207–39.

Wilson JM, Kalasinsky KS, Levey AI, Bergeron C, Reiber G, Anthony RM, Schmunk GA, Shannak K, Haycock JW, Kish SJ. Striatal dopamine nerve terminal markers in human, chronic methamphetamine users. Nature Med 1996;2:699–703.

Xie T, Tong L, Barrett T, Yuan J, Hatzidimitriou G, McCann UD, Becker KG, Donovan DM, Ricaurte GA. Changes in gene expression linked to methamphetamine-induced dopaminergic neurotoxicity. J Neurosci 2002;22:274–83.